Unlocking gas reserves in bypassed stratigraphic traps in a deepwater brownfield using prestack seismic inversion: A case study from offshore Nile Delta, Egypt

Hamed Z. El-Mowafy[1], Mohammed Ibrahim[2], and Dallas B. Dunlap[3]

https://doi.org/10.1190/tle37070502.1.

Abstract

In deepwater depositional systems such as the slope canyon-turbidite channel system encountered on the continental slope of the offshore West Nile Delta Basin, deterministic prestack seismic inversion followed by facies classification using formation microimager facies logs delineated thick-bedded and thin-bedded gas-sand reservoirs encased in bypassed stratigraphic traps. Prestack seismic inversion was applied over the Scarab Field in the West Delta Deep Marine concession to evaluate the hydrocarbon potential of newly identified stratigraphic traps. Three angle stacks were inverted using a simultaneous inversion approach to estimate the elastic properties (P-impedance and V_P/V_S ratio). Using the elastic volumes produced from the inversion, Bayesian facies classification was applied to separate thin- and thick-bedded gas-sand facies from shale. Facies classification was focused on two prospective bypassed stratigraphic traps: the Upper Scarab Channel remnant levees (remnant middle levee [RML] and southern remnant levee) and the Lower Scarab Channel lateral accretion packages (LAPs). A development well location is proposed to validate the interpreted gas-sand reservoirs in the shallower RML and the deeper LAPs stratigraphic traps. The results suggest that application of the prestack seismic inversion and facies classification led to reliable inferences likely to have a positive impact on field development, potential reserves growth, and consequently boosting gas production.

Introduction

The Nile Delta is one of the world's classic delta systems (Figure 1), and its offshore area is rapidly emerging as a major gas province. Offshore exploration using high-quality 3D seismic data helped achieve significant discoveries in the last two decades. The giant Zohr discovery, made in 2015 by the Italian oil company Eni, is proof of the significant remaining hydrocarbon potential of the offshore Nile Delta Basin.

Although fluvial and deltaic reservoirs have long produced oil and gas in Egypt's Western Desert, onshore (El-Mowafy and Marfurt, 2016) and offshore Nile Delta, U.S. gulf coast, and elsewhere, deepwater channel systems and turbidite plays have been the primary focus of hydrocarbon exploration and development. The prolific Pliocene canyon channels offshore Egypt are restricted to the Nile Delta cone. Scarab Field is one of at least nine Pliocene submarine canyon-channel systems in the West Delta Deep Marine (WDDM) concession that were found in the expansive slope setting in a period of progradation of the El-Wastani Formation (H. Z. El-Mowafy, personal communication, 2018).

In the WDDM concession, previous studies (e.g., Mohamed et al., 2014) have focused on characterizing the main channel reservoirs. This study is focused on characterizing bypassed subtle stratigraphic traps encountered in the upper Pliocene El-Wastani Formation in the Scarab gas brownfield (H. Z. El-Mowafy, personal communication, 2018). These bypassed traps are important architectural elements of the submarine deepwater turbidite channel systems.

The Scarab Canyon is occupied by two channel systems, namely the Lower and the Upper Scarab channels. The trapping mechanism is stratigraphic along the eastern, western, and southern limits in the form of pinch-outs and dip closure in the north. Charging of the Pliocene reservoir in the WDDM concession is from the north, and the gas is a mixture of biogenic and thermogenic origin (Mohamed et al., 2017). The Scarab Field gas accumulation is likely controlled by the sealing character of the overlying mass-transport complex (MTC).

Production from the Scarab Field started in March 2003 and reached 800 million standard cubic feet of gas per day for the domestic Egyptian market (Mohamed et al., 2014). The current daily production rate is believed to be declining. It is believed that integrating seismic inversion with facies classification may lead to characterizing bypassed traps, optimizing development plans, and increasing reservoir production.

The prestack algorithm used in this work is constrained sparse spike inversion, which models the input seismic data as the convolution of the seismic wavelet with a reflection coefficient series and imposes additional constraints to limit nonuniqueness in the inverse problems (Debeye and Van Riel, 1990). Through prestack inversion, one can create partial stacks from different angle ranges and invert them, solving simultaneously for an earth model in which three elastic properties (compressional and shear impedances, or V_P/V_S plus density) are consistent across all angle ranges.

Bayesian inference can be used to infer the probabilities of occurrence of geologic facies from seismic reflection data and in particular, prestack inversions. First, one will need to assign joint probability density functions (PDFs) to facies clusters from well log data displayed on crossplot space defined by the inversion outcomes. Second, applying Bayes' rule will provide the probability of occurrence of each of the facies at every location in 3D space and follow immediately the volumes of the most probable facies (Pendrel et al., 2017).

While prestack seismic inversion enhances tuning thickness and provides details of internal reservoir properties, facies classification predicts reservoir facies and provides details of reservoir heterogeneity and architecture.

[1]NeuEra GeoServices, Houston, Texas, USA. E-mail: hamed.elmowafy@neuerageos.com.
[2]CGG, Houston, Texas, USA. E-mail: mohammed.ibrahim@cgg.com.
[3]Bureau of Economic Geology, University of Texas, Austin, Texas, USA. E-mail: dallas.dunlap@beg.utexas.edu.

The aim of this study is to perform seismic reservoir characterization using seismic inversion and facies classification to evaluate the hydrocarbon potential of the bypassed stratigraphic traps interpreted by El-Mowafy et al. (personal communication, 2018) in an effort to extend the economic commercial viability of the Scarab Field.

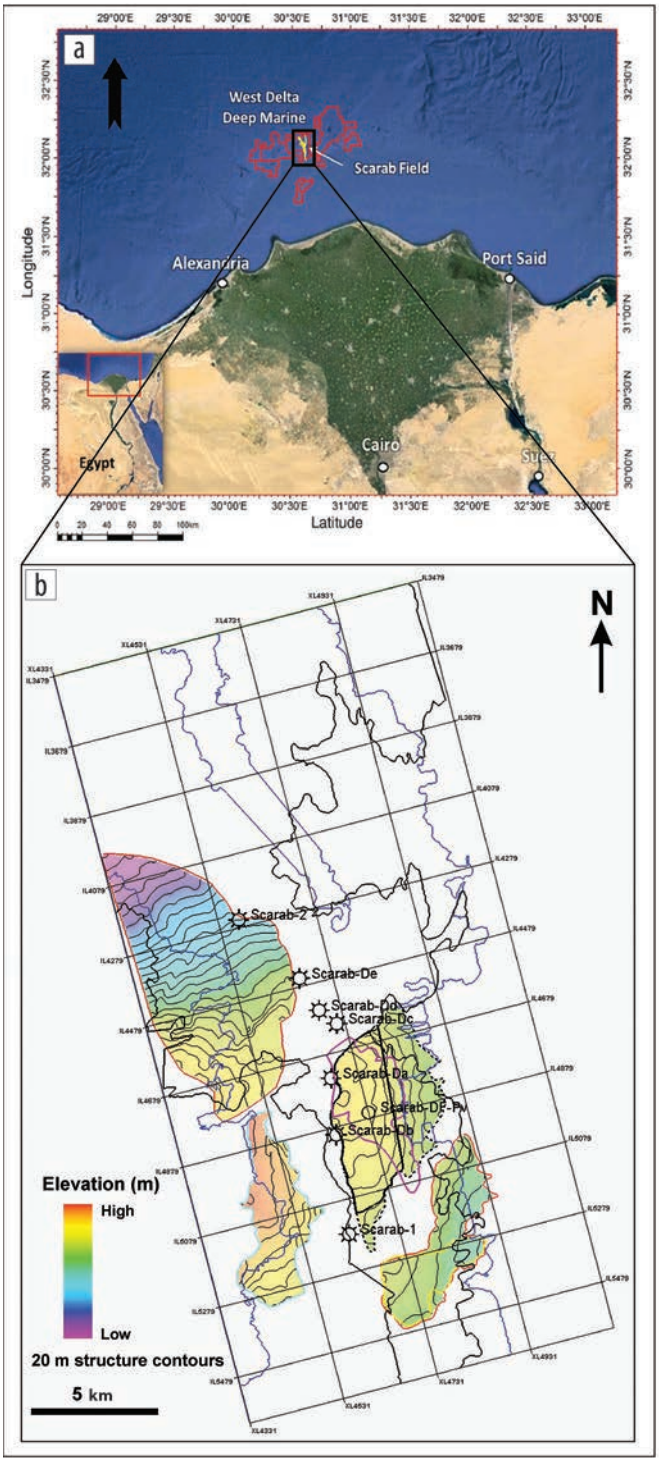

Figure 1. (a) Map of Egypt showing the location of Scarab Field (yellow polygon) in the WDDM concession (red polygons), offshore Nile Delta (modified from Google Earth). (b) Scarab Field zoom-in map showing Lower Scarab Canyon (black polygon), Upper Scarab Canyon (blue polygon), and Upper Scarab bypassed remnant levees (polygons overlain by structure contours). The black dashed polygon delineates a prospective Upper Scarab Channel RML overlapping with Lower Scarab Channel LAPs (unfilled pink polygon). The circle in the middle of the RML represents the surface location of a proposed development well (Scarab-Df-P).

Data and methods

The focus of this study is to use 3D seismic angle stacks and well data to characterize gas-sand reservoirs of upper Pliocene deepwater-bypassed stratigraphic traps and to delineate the boundaries of the sweet spots — the gas-bearing sands encountered in these traps. This is achieved through performing prestack seismic inversion and using the inversion outputs for the estimation of rock facies.

The data sets available for this study include a full-stack prestack time migration 3D seismic volume and three partial-angle stacks of near (0°–15°), mid (15°–30°), and far (30°–45°) angles with a recorded duration of 3 s and sampled at 4 ms. The signal-to-noise ratio is average, with a vertical resolution in the focus interval of interest of about 12 m (39 ft). Seismic data conditioning was applied to remove noise and to correct time misalignment.

Seven wells drilled in the Scarab Field produce hydrocarbons from turbidite channel sands. All the wells are vertical and have a full suite of wireline logs over the Scarab reservoir interval. Interpreted formation microimager (FMI) facies are available for all Scarab Field wells and were used as an input for seismic facies classification.

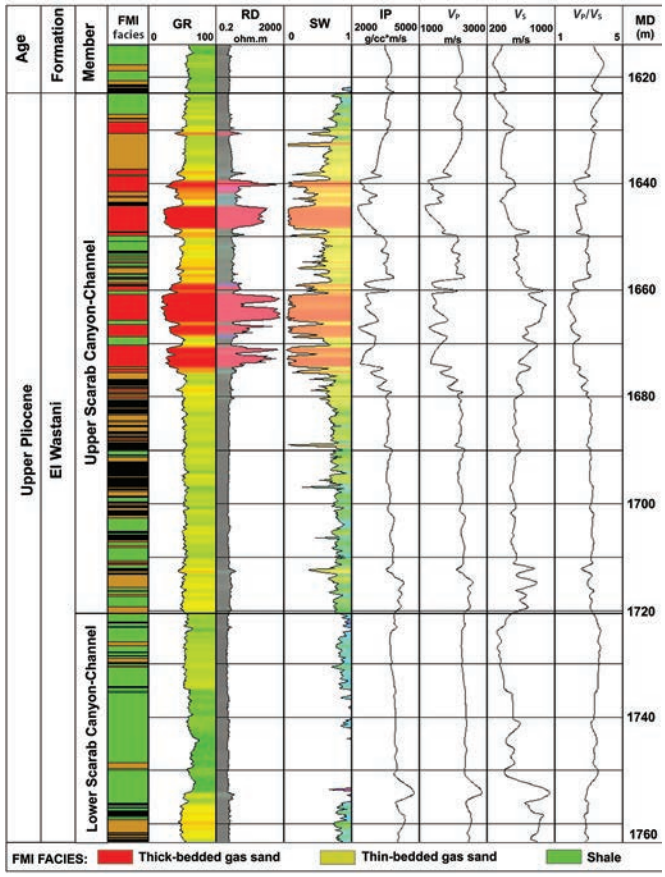

Figure 2. Type log of the Scarab-Da well showing the stratigraphy and well logs of the El-Wastani Formation in Scarab Field, WDDM concession. Interpreted FMI facies are also shown. Compared with the Upper Scarab Canyon Channel, the Lower Scarab Canyon Channel at this well location is dominated by shale and thin-bedded sand.

The seven wells were tied to the full-stack seismic with a consistent correlation. Three wavelets were estimated from the seismic amplitude of near, mid, and far stacks along with the wells that have adequate logging length. Wavelets are key components in inversion workflows and have a significant effect on the inversion results. The wavelets were inspected and ensured stable amplitude and phase spectra over the seismic frequency band. In addition, the wavelets were validated by comparing the synthetic from the convolution models against the seismic amplitude of the partial-angle stacks. The extracted wavelet has a length of 140 ms and a phase of about 180°.

Five horizons were interpreted, representing top remnant levees, top Upper Scarab Channel, base Upper Scarab Channel, top Lower Scarab Channel, and base Lower Scarab Channel. These horizons were used to create the low-frequency model and to interpret the inversion results.

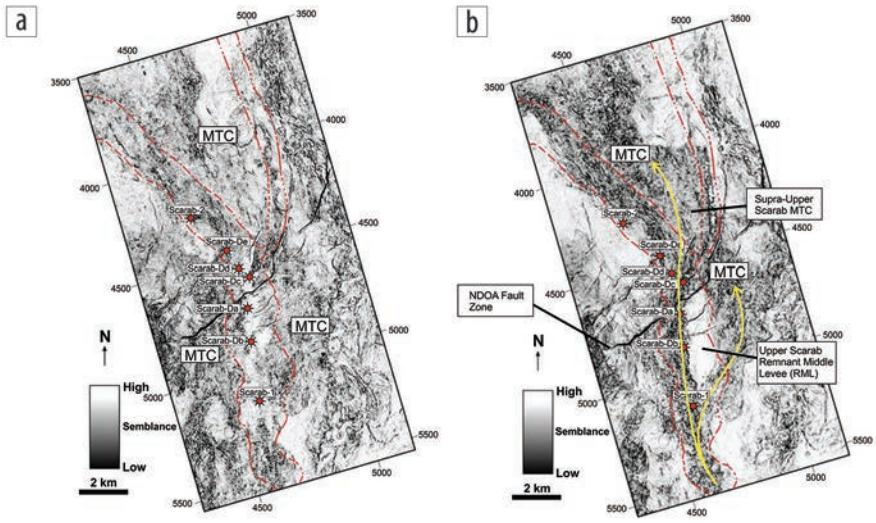

Figure 3. (a) Flattened coherency slice 80 ms above top Upper Scarab Channel. The MTC is draping and eroding the Scarab Channel and levee sequences and acts as an efficient seal for the underlying levees and channel gas-sand reservoirs. (b) Flattened coherency slice 56 ms above top Upper Scarab Channel highlighting preserved levee deposits. The remnant Scarab levees are interpreted as bypassed stratigraphic traps potentially sealed at the top and laterally by the MTC deposits and the NDOA Fault. Upper Scarab Canyon boundaries (red polygons) are shown on the maps. The well locations are approximately aligned parallel to the Upper Scarab Channel thalweg line (the line that connects the lowest points in the channel).

Seismic data is band limited by nature; thus, the inversion process will yield relative elastic properties. To allow the inversion algorithm to generate absolute elastic properties (P-impedance and V_P/V_S), one must add the low-frequency information to the seismic inputs to fill the gap in frequency below the seismic band and to generate absolute volumes that can yield a quantitative interpretation of reservoir properties. Interpolating log curves between wells guided by structural framework (horizons and faults) and optionally using external attributes is the traditional approach to building low-frequency models. In this work, we apply a different approach to avoid errors or artifacts that may arise from the interpolation method during the process. The low-frequency model was built initially from a 3D shale trend followed by a first-pass inversion (Jarvis, 2006). Using the first-pass inversion results, the sand geobodies embedded in the shale were captured, and the 3D trend was updated. Iteratively, the process of inversion and capturing the geobodies was repeated until a reasonable final 3D low-frequency model was generated. No interpolation between wells was used at any time during the process of building the 3D model. The prestack seismic inversion typically yields volumes of P-impedance, V_P/V_S, and density. However, the inverted density results were believed to be of poor quality and were not used in analysis or interpretation moving forward.

Remaining potential of the Scarab gas brownfield

El-Mowafy et al. (personal communication, 2018) performed seismic sedimentological analysis, described the 3D evolution of the Scarab slope canyon-channel systems, and identified four potential bypassed stratigraphic traps: (1) Upper Scarab Channel remnant levees, (2) Lower Scarab Channel lateral accretion packages (LAPs), (3) Lower Scarab Channel pinch-outs, and (4) Lower Scarab Channel lateral splays. Such traps may represent development and production opportunities in the mature Scarab gas field and could be potential analogs for similar stratigraphic traps in the WDDM concession and the Eastern Mediterranean Basin. Prestack seismic inversion and facies classification were performed to delineate reservoir-quality gas sand contained in these traps. The focus of this paper is on characterizing two traps: the Upper Scarab Channel remnant levees and the Lower Scarab Channel LAPs.

Upper Scarab Channel: Bypassed remnant levee traps. Four remnant levees were identified on both sides of the Upper Scarab Channel and are described as isolated stratigraphic traps sealed vertically and laterally by the nonreservoir deposits of the Scarab MTC (H. Z. El-Mowafy, personal communication, 2018). Regarding turbidite channel sands, the Scarab Field gas accumulation is likely controlled by the sealing character of the overlying MTC. Similarly, the remnant levees (e.g., remnant middle levee [RML]) are also interpreted to be sealed by the deposits of the same MTC. The preserved remnant levees of the Upper Scarab Channel (Figures 3 and 4) are sitting above the Upper Scarab Channel gas-water contact (GWC) and likely separated from the underlying Upper Scarab Channel sand reservoir facies by passive channel-fill deposits.

Thin-bedded turbidites have been uncommon primary targets for hydrocarbon field development because most deepwater operators have focused on testing sand-rich channel-fill deposits. However, thin-bedded turbidites can contain large amounts of sand, of which individual beds can be laterally continuous, and hence can make significant secondary reservoir targets (Hansen et al., 2015).

The geologic model in the study area predicts high net/gross sand ratio in the proximal remnant levees and decreases away from channel flanks. No wells penetrated the bypassed stratigraphic traps identified by El-Mowafy et al. (personal

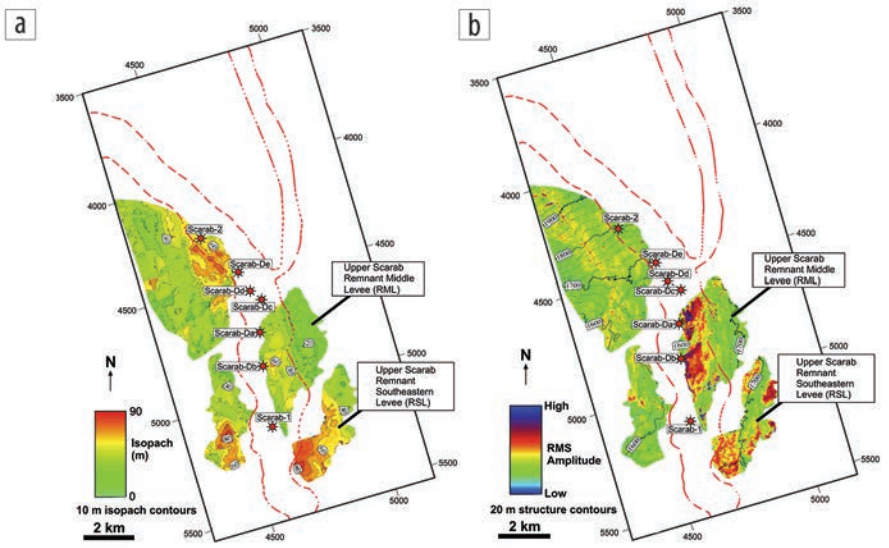

Figure 4. (a) Isopach map of the Scarab remnant levees demonstrating changes in the preserved thickness from proximal to distal settings. Note the well-developed thickness of the proximal middle levee (RML) and RSL. (b) rms amplitude map extracted between top remnant levees and top Upper Scarab Channel overlaid by top levees structural contours. The RML and RSL exhibit high rms seismic amplitudes compared with the two levees on the western channel flank.

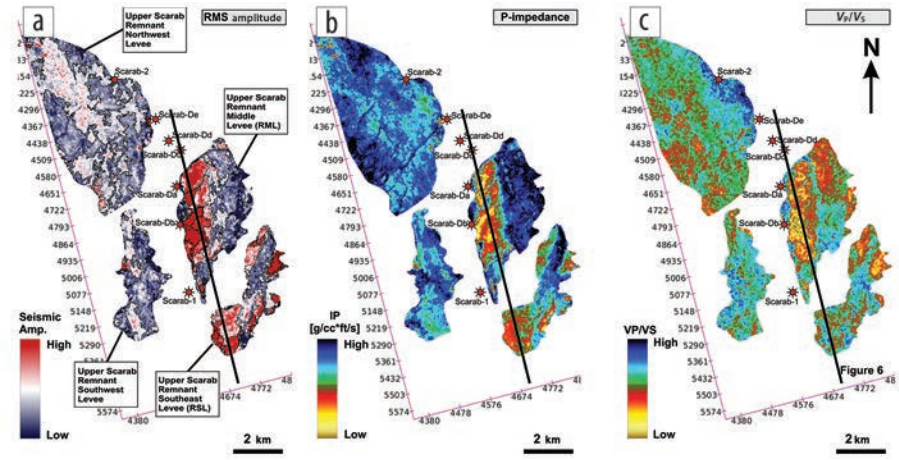

Figure 5. Extraction maps for the interval between top remnant levees and top Upper Scarab Channel for (a) rms seismic amplitude, (b) inverted P-impedance, and (c) inverted V_P/V_S ratio. The RML and RSL exhibit high rms seismic amplitudes in (a). The low-moderate P-impedance (hot color) values (b) and V_P/V_S (hot color) values confirm the rms anomalies in (a). These anomalies are interpreted to be related to the presence of gas-sand reservoirs and to variations in the net/gross ratio.

communication, 2018). The closest wells to the RML stratigraphic trap (Figure 1b) are Scarab-Db and Scarab-Da. Levee deposits have been documented by many workers to contain reservoir-quality thin-bedded sandstones. These types of thin-bedded sandstone deposits have been described as low-resistivity pay zones. Such pay zones would be best developed in proximal levee settings (Clemenceau et al., 2000).

The flattened coherency slice extracted at 56 ms above the Upper Scarab Channel sequence (Figure 3) clearly highlights the Upper Scarab RML, exposed as a result of erosion and emplacement of the MTC. Four remnant levee segments were interpreted with structure, and isopach maps were generated for the Scarab remnant levees (Figure 4). The levees demonstrate changes in the preserved thickness from proximal to distal settings. Note the well-developed thickness of the proximal middle levee (RML) and southern remnant levee (RSL). Of the four remnant levees, the RML is the most prospective compartment because it exhibits the highest rms amplitude anomalies relative to other remnant levee segments (Figure 4b). This bypassed RML stratigraphic trap is interpreted to be sealed laterally and at the top by the MTC deposits and is probably sealed on its northern boundary by the Nile Delta Offshore Anticline (NDOA) Fault (Figures 3 and 4b). The RSL also exhibits high rms amplitude anomaly (Figure 4b).

Thus, one of the motivations of this study is to understand the high rms amplitude anomalies of the remnant levees through prestack seismic inversion and facies classification workflow. Low-moderate P-impedance and V_P/V_S ratio values, which are typical to that rock type of reservoir, are observed for the remnant levees as seen in Figures 5b and 5c, and confirm the high rms seismic-amplitude anomalies in Figure 5a. A northwest to southeast arbitrary line shows the variations in P-impedance (Figure 6c) and V_P/V_S ratio (Figure 6d) along the proximal levees near the Upper Scarab Channel flank. Pay zones would be best developed in proximal levee settings. The RML gas-sand deposits seem to taper and probably become finer grained laterally away from the Upper Scarab Channel (Figures 4b, 5, and 7a).

The penetrated section of the Upper Scarab Channel in the Scarab-Da and Scarab-Db wells — the closest two wells to the prospective RML (Figures 3, 4, and 5) — contains a thick succession of reservoir-quality (porosity: 15% to >25%) thick-bedded and thin-bedded gas sands interbedded within silt and shale levee complex facies.

The total area of the RML preserved on the Upper Scarab Channel eastern flank is 10.38 km^2 (4.02 mi^2). The area of the most prospective proximal part of the RML, defined by the consistent rms, P-impedance, and V_P/V_S anomalies, is 4.5 km^2 (1.74 mi^2). The total area of the RSL segment (Figures 4 and 5) is 6.35 km^2 (2.45 mi^2) and the prospective area of this RSL is 3.0 km^2 (1.17 mi^2).

The structural relief of the RML is about 100 m (328 ft) (Figure 4b). The RML thickness within the area covered by the structurally closed contours and by seismic attribute anomalies ranges from 20 to 60 m (66 to 197 ft), and the thickness of the

anomalous proximal part of the RML ranges from 40 to 60 m (131 to 197 ft) (Figures 4–6). The four remnant levees lie above the GWC in the Scarab Field. All the wells drilled to date in Scarab Field did not penetrate the RML and RSL, and as such they are considered as potential gas-bearing bypassed stratigraphic traps in the mature Scarab gas field.

Lower Scarab Channel: Lateral accretion packages trap. LAPs associated with the Lower Scarab Channel are the second bypassed stratigraphic trap identified in the Scarab Field area (H. Z. El-Mowafy, personal communication, 2018). LAPs are a characteristic suite of deposits with a distinctive arrangement and structure, deposited laterally during channel meandering (Allen, 1982). Channel deposits are the sediments accumulated near the main channel and in bar complexes. LAPs can develop by fluvial or submarine processes.

About five distinguishable LAPs can be seen inside the Lower Scarab Channel meander loop (Figure 7b). Low-moderate P-impedance and V_P/V_S values are estimated for the LAPs as seen in Figures 7b and 7c and are similar to the RML impedance anomalies in Figure 7a. A northeast to southwest arbitrary line tied to the Scarab-Db well is showing variations in the P-impedance (Figure 8b) and V_P/V_S (Figure 8c) attributes for both the shallower RML and the deeper LAPs reservoirs. The P-impedance and the V_P/V_S anomalies may indicate the presence of reservoir-quality gas sand in the RML and the LAPs traps, and could be stacked as two targets to be tested by a new development well (Scarab-Df-Proposed) (Figure 8). In this case, the Scarab-Df-P well can be drilled to reach the base of the shallower RML secondary reservoir target, acquire necessary well log suites, and perform petrophysical evaluation. It can continue drilling to the proposed total depth at the base of the deeper LAPs primary reservoir target, acquire well logs, and evaluate pressure data and flow rates of the primary and secondary reservoir targets. Completion procedures will be based on test results.

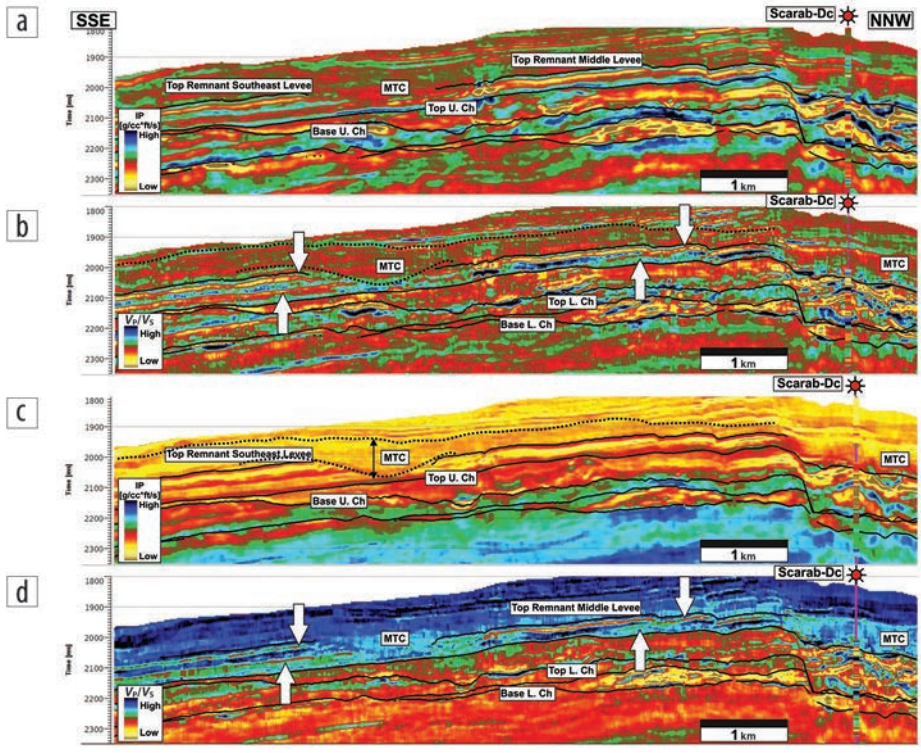

Figure 6. (a) Northwest–southeast relative P-impedance section, (b) relative V_P/V_S ratio, (c) full-band P-impedance section, and (d) full-band V_P/V_S section showing the anomalies of the RML and RSL deposits (white arrows) preserved on the eastern flank of the Upper Scarab Channel. From the impedance and V_P/V_S sections, the RML appears to have better proximal facies quality and continuity compared to the RSL. Note that the MTC deposits are interpreted to be the seal for underlying Upper Scarab Channel sands and remnant levees. Location of the section is shown in Figure 5.

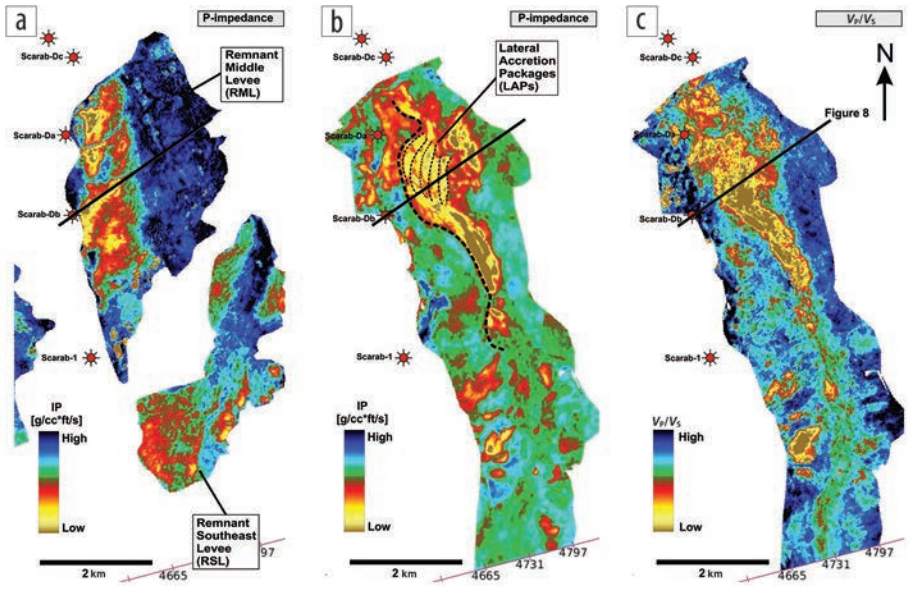

Figure 7. (a) P-impedance map, extracted for the interval between top remnant levees and top Upper Scarab Channel, showing anomalies in the proximal RML and RSL traps. (b) Anomalous low-moderate impedance values of the Lower Scarab Channel and the associated interpreted LAPs overlap with the shallower proximal RML trap in (a). (c) V_P/V_S map of the LAPs, which confirms the P-impedance anomalies in (b).

The total area of the LAPs and the associated southern high-amplitude Lower Scarab Channel segment (Figures 7b and 7c) is approximately 4.5 km^2 (1.74 mi^2), and their combined vertical thickness is approximately 64 m (210 ft). No wells drilled into the LAPs stratigraphic trap, which represents a promising development opportunity in the mature Scarab gas field. Preliminary

reserve estimates of the combined gas-initial-in-place (GIIP) from the two targets (RML and LAPs) is approximately ±128 BCF (mean case). Geostatistical seismic inversion work is in progress for more accurate reserve estimation.

The north-south facies and attributes sections extracted along the anomalous proximal part of the RML (Figure 9) reflect the presence, continuity, and quality of the shallower RML and deeper LAPs reservoirs. Based on observations from inversion attributes, the RML and deeper LAPs traps are vertically overlapping (Figures 8 and 9), contain reservoir-quality gas-sand facies, and can be considered as prospective drilling targets. Figure 8 shows a schematic of the proposed well location.

Bayesian facies classification

Lithology and fluid prediction is important both in exploration and development of deepwater reservoirs. Bayesian classification is a technique used to infer the probabilities of the occurrence of lithology and/or fluid from seismic inversion.

Four clusters of facies were identified from the FMI logs of the Scarab wells, which include thick-bedded gas sands, thin-bedded gas sands, brine sands, and shale lithologies. Rather than using petrophysical log facies, the FMI facies of the Scarab wells — which are usually used in reservoir geomodeling and simulation — are used in this study with inversion results to generate facies probability volumes for the RML, RSL, and LAPs. Crossplots were constructed from well log P-impedance and V_P/V_S ratio, which are similar to those attributes driven from seismic inversion and color coded by the FMI facies (Figures 10b and 10c). Figure 10a shows three joint PDFs assigned to each facies that were used to drive the probability volume of each facies. The probability of the brine or water sand is not included in this study. Red points on the crossplot (Figure 10a) represent thick-bedded gas sand, brown points represent thin-bedded gas sand, and green points represent shale facies.

A stratigraphic slice 16 ms below the top levees horizon is shown in Figure 11. The dominance of the P-impedance and V_P/V_S anomalies in Figures 11b and 11c are interpreted to infer thick-bedded and thin-bedded gas-sand facies (red and brown facies). It also may indicate overall high net/gross sand ratio in the proximal RML trap.

The upper panel in Figure 12 is a cross section showing the distribution of facies, which include the thick-bedded (red) and thin-bedded (brown) gas-sand facies, and shale facies (green) encountered in the RML, Upper Scarab Channel, and Lower Scarab Channel. Note the well-developed LAPs in the Lower Scarab Channel along the cross-section line. The ongoing geostatistical seismic inversion is expected to enhance the resolution and net pay, especially in the RML. The middle panel shows the probability distribution of the thick-bedded gas-sand facies. The probability distribution of the thin-bedded gas-sand facies is also shown in the lower panel (Figure 12).

The presence of thick-bedded and thin-bedded gas sands, silt, and shale within the RML complex bedding architecture apparently might be expected to reduce reservoir connectivity and

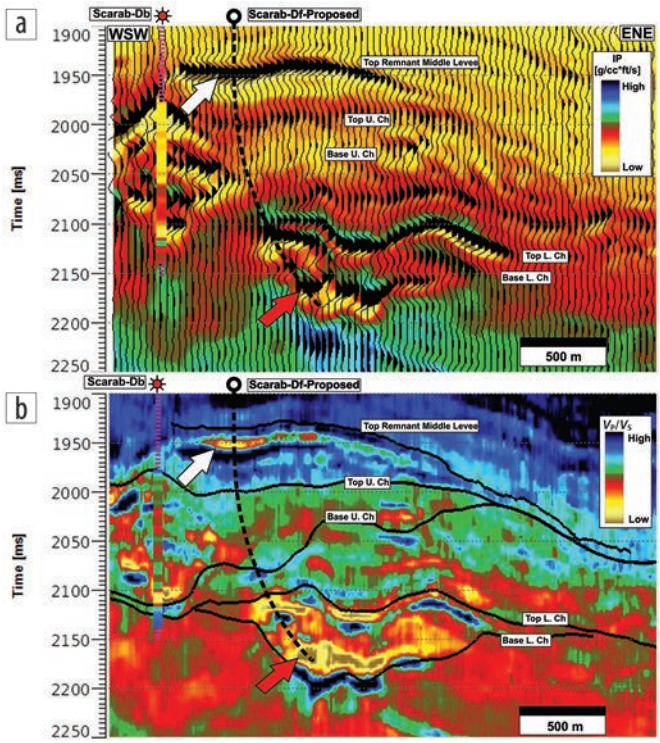

Figure 8. (a) West-northwest–east-southeast P-impedance section overlaid by seismic wiggles, and (b) V_P/V_S section showing the anomalies of the shallower laterally extensive RML beds (white arrows) and the deeper LAPs (red arrows). Schematic (black dashed line) location of the proposed development well to test both objectives is shown. Location of the section is shown in Figure 7.

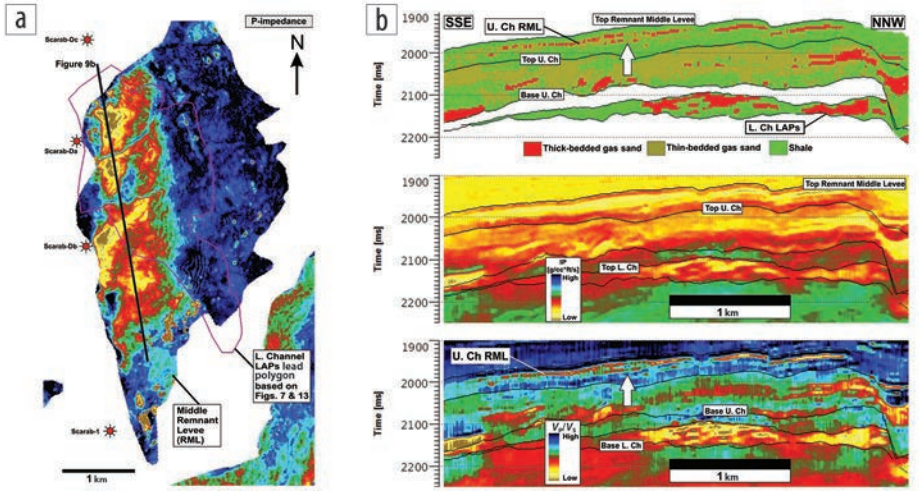

Figure 9. (a) P-impedance map for the prospective Upper Scarab RML showing vertical overlap with the deeper Lower Scarab LAPs delineated by the pink polygon. (b) South-southeast–north-northwest section along the proximal levee showing the character of the RML and the LAPs reservoirs from facies classification — explained in the next section (upper panel), P-impedance (middle panel), and V_P/V_S (lower panel). White arrows point to multiple laterally extensive thick- and thin-bedded gas-sand beds in the RML, which may contain significant hydrocarbon volumes. Line of section is shown in Figure 9a.

decrease well flow rate and recovery. Although there is a potential for lateral and vertical connectivity and pressure communication across the proximal RML reservoirs (Figures 8, 9, 11, and 12), a side track could be drilled in the proximal RML sequence to better enhance connectivity and flow. The 3D connectivity could be enhanced by a biological activity in the proximal levee and by the potential presence of a small subseismic sand-filled overbank channel cut into the obliquely dipping RML thick-bedded and thin-bedded gas sands.

A Bayesian facies classification exercise was also performed for the deeper LAPs bypassed stratigraphic trap. The facies slice extracted at 32 ms below top Lower Scarab Channel indicates the dominance of the thick-bedded gas-sand facies in the Lower Scarab Channel LAPs (Figure 13a). Brown facies represent thin-bedded gas sand, and the green background color represents shale facies. Figure 13b is the probability of occurrence of thick-bedded facies extracted at the same level as Figure 13a. The LAPs anomalies on the P-impedance (Figure 13c) and V_P/V_S (Figure 13d) slices are consistent with the facies slice in Figure 13a and probability slice in Figure 13b at this stratigraphic level.

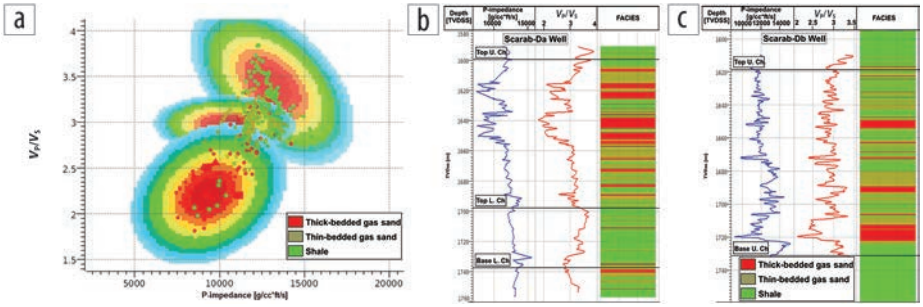

Figure 10. (a) Crossplot of P-impedance versus V_P/V_S ratio using data from (b) Scarab-Da and (c) Scarab-Db wells. Reservoir lithologies are defined using FMI facies. The constructed joint PDF ellipses: red points represent thick-bedded gas sand (lower PDF ellipse), brown points represent thin-bedded gas sand (middle PDF ellipse), and green points represent shale facies (upper PDF ellipse). The FMI facies and the calculated P-impedance and V_P/V_S curves for the Scarab-Da and Scarab-Db wells are shown in (b) and (c), respectively.

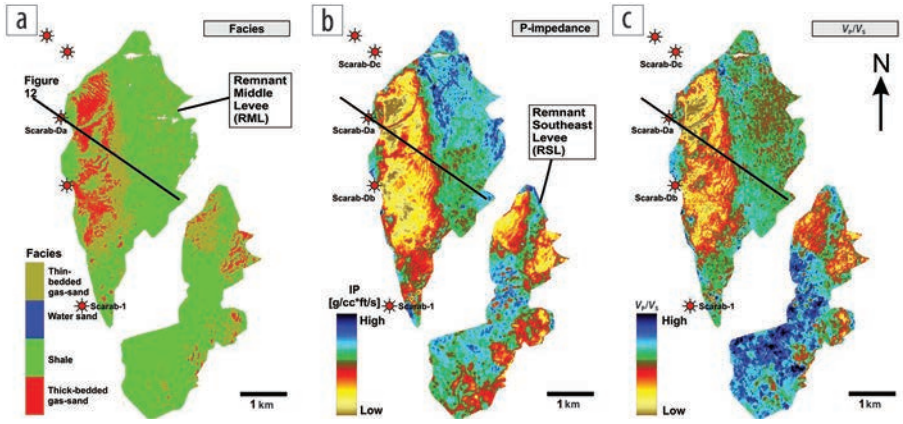

Figure 11. (a) Facies classification stratal slices 16 ms below top levees showing the RML and RSL segments. Note the abundant thick-bedded gas-sand facies (red facies in [a]), which may also infer high net/gross sand ratio in the proximal part of the levee. Brown facies represent thin-bedded gas sand. The equivalent (b) P-impedance and (c) V_P/V_S ratio maps of the RML and RSL show anomalies consistent with the probability facies in (a). Line of section connecting the Scarab-Da well is shown in Figure 12.

Results presented in Figures 11–13 indicate the presence of reservoir-quality gas sand in the Upper Scarab RML and Lower Scarab LAPs contained in the bypassed stratigraphic traps, and could be stacked as two targets to be tested by the proposed development well (Scarab-Df-P) (Figures 8 and 12).

Conclusions and recommendations

Deterministic prestack seismic inversion was applied to Scarab 3D seismic data to characterize bypassed stratigraphic traps identified in the Scarab slope canyon-channel systems. Facies classification using the seismic inversion and Scarab FMI logs delineated the thick-bedded and thin-bedded gas sand encased in the bypassed remnant levees (RML and RSL) and in LAPs traps. The delineated RML bypassed stratigraphic trap is interpreted to contain thick-bedded and thin-bedded gas-sand facies sealed laterally and vertically by the MTC nonreservoir facies. The gross thickness of the most prospective proximal RML stratigraphic trap ranges from 40 to 60 m (131 to 197 ft). The total area of the RML is approximately 10.4 km^2 (4.0 mi^2), and the area of the most prospective part of the RML is approximately 4.5 km^2 (1.74 mi^2). The second bypassed stratigraphic trap is the LAPs associated with the Lower Scarab Channel. It occupies an area of approximately 4.5 km^2 (1.74 mi^2). The gross thickness of the LAPs is estimated as ~64 m (210 ft).

The remnant levees (RML and RSL) and the LAPs subtle stratigraphic traps appear to have the potential to add gas reserves in the Scarab brownfield. These traps could be tested by drilling the new proposed development well that is expected to boost gas production from the Scarab Field. The estimated mean GIIP from the deeper primary LAPs target reservoir and the shallower secondary RML target reservoir is ±128 BCF. Such bypassed subtle traps can also serve as an analogy to explore and develop similar reservoirs in the Pliocene gas play in the offshore West Nile Delta, Mediterranean Basin, and elsewhere.

Geostatistical seismic inversion is expected to provide better reserve estimation and better understanding of the compartmentalization and connectivity of the Scarab reservoirs. This may help in identifying untapped and/or incompletely drained compartments within the Scarab Canyon channels. TLE

Acknowledgments

The authors thank the Egyptian General Petroleum Corporation and Rashid Petroleum Company (RASHPETCO) for providing the data and for their permission to publish this study. We would like to thank Islam A. Mohamed from RASHPETCO and Mosab Nasser from LEAN GeoSolutions for their thoughts and fruitful discussions during the course of this work.

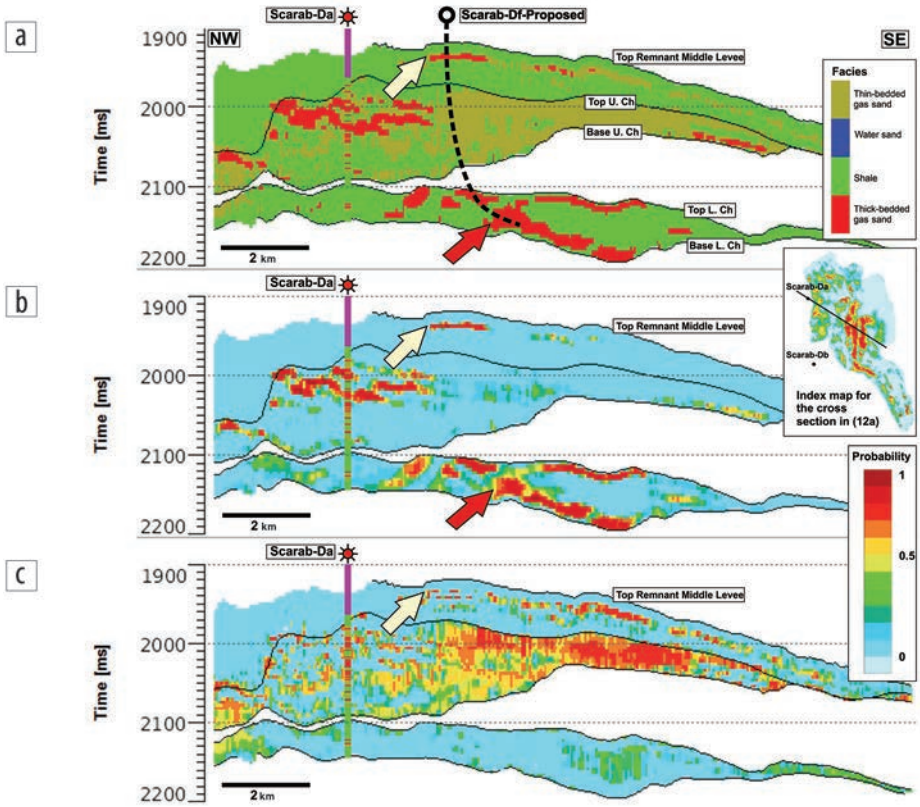

Figure 12. (a) Northwest–southeast facies classification section through Scarab-Da well showing the distribution of the thin-bedded (brown) and thick-bedded (red) gas-sand facies in the wedge-shaped RML, Upper Scarab Channel, and Lower Scarab Channel. (b) Probability distribution of thick-bedded gas-sand facies. (c) Probability distribution of thin-bedded gas-sand facies. White arrows refer to thick- and thin-bedded RML gas-sand facies. Red arrows refer to thick-bedded LAPs gas-sand facies. Location of the cross section is shown in Figure 11.

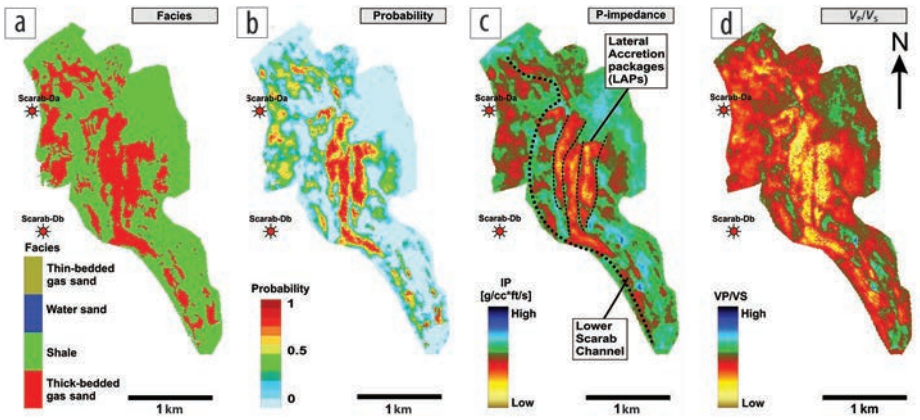

Figure 13. (a) Facies classification stratal slices, 32 ms below top Lower Scarab Channel, showing the dominance of the thick-bedded gas-sand facies in the Lower Scarab Channel LAPs. (b) Red facies represent thick-bedded gas sand. Anomalies on the equivalent (c) P-impedance and (d) V_P/V_S ratio maps of the LAPs are consistent with the probability facies in (a) and (b).

Corresponding author: hamed.elmowafy@neuerageos.com

References

Allen, J. R. L., 1982, Sedimentary structures, their character and physical basis: Developments in Sedimentology: Elsevier.

Clemenceau, G. R., J. Colbert, and D. Edens, 2000, Production result from levee-overbank turbidite sands at Ram/Powell Field, deepwater Gulf of Mexico: 20th Annual Research Conference, Gulf Coast Section SEPM, 241–251.

Debeye, H. W. J., and P. Van Riel, 1990, L_p-norm deconvolution: Geophysical Prospecting, **38**, no. 4, 381–403, https://doi.org/10.1111/j.1365-2478.1990.tb01852.x.

El-Mowafy, H. Z., and K. J. Marfurt, 2016, Quantitative seismic geomorphology of the middle Frio fluvial systems, south Texas, United States: AAPG Bulletin, **100**, no. 4, 537–564, https://doi.org/10.1306/02011615136.

Hansen, L., R. Callow, I. Kane, F. Gamberi, M. Rovere, B. Cronin, and B. Kneller, 2015, Genesis and character of thin-bedded turbidites associated with submarine channels: Marine and Petroleum Geology, **67**, 852–879, https://doi.org/10.1016/j.marpetgeo.2015.06.007.

Jarvis, K., 2006, Integrating well and seismic data for reservoir characterization: Risks and rewards: Presented at Australian Earth Science Convention.

Mohamed, I. A., H. Z. El-Mowafy, D. Kamel, and M. Heikal, 2014, Prestack seismic inversion versus neural-network analysis: A case study in the Scarab Field offshore Nile Delta, Egypt: The Leading Edge, **33**, no. 5, 498–506, https://doi.org/10.1190/tle33050498.1.

Mohamed, I. A., O. Shenkar, and H. Mahmoud, 2017, Understanding reservoir heterogeneity through water saturation prediction via neural network — A case study from offshore Nile Delta: The Leading Edge, **36**, no. 4, 298–303, https://doi.org/10.1190/tle36040298.1.

Pendrel, J., H. Schouten, and R. Bornard, 2017, Bayesian estimation of petrophysical facies and their applications to reservoir characterization: 87th Annual International Meeting, SEG, Expanded Abstracts, 3082–3086, https://doi.org/10.1190/segam2017-17588007.1.